Cellulose (2022) 29:4021–4037
https://doi.org/10.1007/s10570-022-04462-4

ORIGINAL RESEARCH

Robust ZnO/HNTs-based superhydrophobic cotton fabrics with UV shielding, self-cleaning, photocatalysis, and oil/water separation

Wei Xu · Lihui Xu · Hong Pan · Keting Li · Jun Li · Liming Wang · Yong Shen · Yangchun Liu · Tianyang Li

Received: 15 October 2021 / Accepted: 27 January 2022 / Published online: 19 March 2022

Abstract In this work, robust superhydrophobic cotton fabrics with ultraviolet (UV) shielding, self-cleaning, photocatalysis, and oil/water separation were successfully prepared based on micro/nano hierarchical ZnO/HNTs (halloysite nanotubes) hybrid particles and silicone elastomer polydimethylsiloxane (PDMS). ZnO/HNTs hybrid particles were prepared by in-situ growth of ZnO nanoparticles on the surface of halloysite nanotubes (HNTs). ZnO/HNTs hybrid particles and PDMS were used to successively coat cotton fabrics by dip-coating approach. The coated cotton fabrics displayed excellent superhydrophobicity with a water contact angle (WCA) of $162.5 \pm 1.0°$ owing to the roughness provided by micro/nano hierarchical ZnO/HNTs hybrid particles and low surface energy achieved by PDMS. After being exposed to the UV lamp for 5 h, about 90.8% of the methylene blue was degraded, indicating that the coated cotton fabrics had excellent photocatalytic activity. The as-prepared cotton fabrics also displayed outstanding self-cleaning and antifouling properties. In addition, due to both superhydrophobic and superoleophilic characteristics, the as-prepared cotton fabrics could be used to separate several oil/water mixtures and showed good recoverability. The superhydrophobic cotton fabrics also exhibited excellent UV shielding performance with a large ultraviolet protection factor (UPF) of 1643.28 due to strong ultraviolet-absorption, light scattering and frequent light reflection of ZnO nanoparticles from ZnO/HNTs composites coated on cotton fabrics. Importantly, the as-prepared cotton fabrics retained superhydrophobic performance after 2000 cycles rubbing, 90 h UV illumination, and immersing in acidic and alkali solutions with different pH values ranging from 1 to 14 for 1 h. These characteristics made multifunctional cotton fabrics a satisfactory candidate in various promising fields.

W. Xu · L. Xu (✉) · H. Pan · K. Li · J. Li · L. Wang · Y. Shen · Y. Liu · T. Li
School of Textiles and Fashion, Shanghai University of Engineering Science, Shanghai 201620, People's Republic of China
e-mail: xulh0915@163.com

Graphical abstract

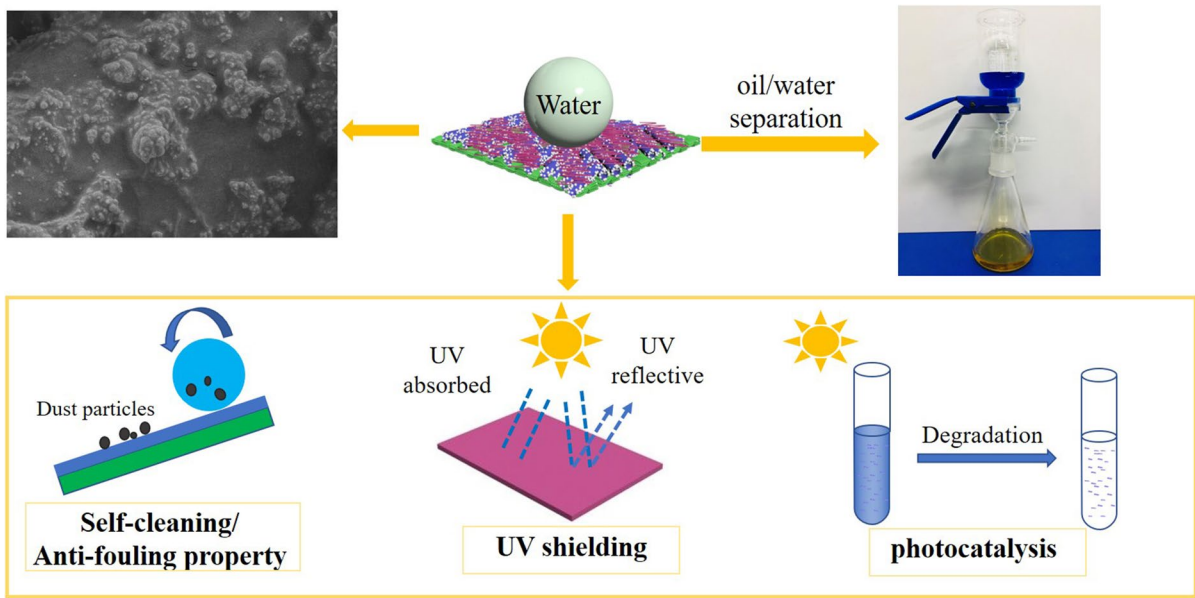

Keywords Superhydrophobic · ZnO/HNTs hybrid particles · Self-cleaning · Photocatalysis · UV shielding · Oil/water separation · Cotton fabrics

Introduction

Cotton fabrics, one of the most common natural cellulosic fabrics, are used in costume, household textiles, and outdoor protection because of their softness, low cost, air permeability and environmental friendliness. Unfortunately, the cotton fabrics could be easily wetted and contaminated by liquids such as water and cola owing to the great number of surface hydroxyl groups on the cellulose fibers of cotton fabrics (Zhou et al. 2018). It had been demonstrated that introduction of superhydrophobicity was a simple and effective strategy to overcome the above-mentioned disadvantages (Xu et al. 2020; Yang et al. 2019a, b, c; Yang et al. 2018).

Inspired by lotus leaves, many researches confirmed that the preparation of superhydrophobic surfaces required the coordination of hierarchical micro/nano structures and ultralow surface free energy (Zhang et al. 2019; Shishodiaa et al. 2019; Tu et al. 2017). The large number of methods had been developed to prepare artificial superhydrophobic surfaces, such as layer-by-layer self-assembly technique (Lin et al. 2018; Jiang et al. 2017), deposition method (Rezaei et al. 2014; Gang et al. 2017), sol–gel method (Zhang et al. 2017a, b; Banerjee et al. 2015), and spray method (Gao et al. 2017). However, to construct superhydrophobic surfaces, the fluoro compounds with ultralow surface energy are widely used, and they display excellent repellence to a wide range of liquids such as water, milk and cola (Kim et al. 2018; Ma et al. 2017; Wang et al. 2019). Unfortunately, the expensive long-chain perfluoroalkyl materials have a potential environmental risk due to difficult biodegradation, long-distance migration, and high bioaccumulation (Zuo et al. 2018; Martin et al. 2003a, b; Cao et al. 2016). Recently, polydimethylsiloxane (PDMS) is an ideal candidate for the fabrication of superhydrophobic surface owing to its low surface energy, environmental friendliness, strong adhesion, and excellent chemical, thermal stability. Cao et al. reported an environmentally friendly strategy to prepare robust superhydrophobic fabrics by dipping in silica aerogel (ormosil) solution and PDMS solution respectively, which possessed self-cleaning and oil–water separation property (Cao et al. 2016). Zheng et al. studied a

self-assembly approach to prepare conductive superhydrophobic cotton fabrics, which employed carboxylated and aminated multiwalled carbon nanotubes to create hierarchical roughness with modification with PDMS (Zheng et al. 2019).

Moreover, for preparation of superhydrophobic surfaces, the construction of these micro/nano hierarchical structures often depends on synthetic nanoparticles (Lin et al. 2017; Jin et al. 2018), etching (Wen et al. 2017; Kim et al. 2007), and template (Jin et al. 2005). These building blocks applied for superhydrophobic coatings are often costly, complicated in process, and may easily cause environmental pollution problems, restricting broader applications. Superhydrophobic surfaces based on naturally occurring nanomaterials are strongly advocated, but so far, only a very few superhydrophobic coatings with natural nanomaterials have been developed. Zhang et al. obtained waterborne nonfluorinated superhydrophobic coatings based on natural nanorods, palygorskite (PAL), followed by methyl polysiloxane modification with polyurethane (PU) as the adhesive layer (Zhang et al. 2017a, b). Qu et al. fabricated superamphiphobic materials by employing kaolin particles and silanes (Qu et al, 2018). HNTs (halloysite nanotubes) is a kind of natural aluminosilicate clay mineral with unique needlelike microstructure. The one-dimensional structure, large surface area, low cost, and tunable surface chemistry of HNTs could benefit for their application in the construction of organic–inorganic nanohybrid materials (Ma et al. 2018). The re-entrant structure could be formed when nanoparticles were introduced on surfaces of HNTs, resulting in rod-dot hybrid particles. Hierarchical micro/nano structures could be generated when a great number of rod-dot hybrid particles aggregated and/or stacked, and the vacancies or pores may be filled with air, showing the potential for water repellency. Liu et al. reported a facile surface coating technique to fabricate superamphiphobic protein-based films materials based on fluorinated HNTs/SiO_2 particles (Liu et al. 2019). The micro/nano hierarchical HNTs/SiO_2 particles were prepared via in-situ growth of SiO_2 on the surface of HNTs through the sol–gel method.

ZnO nanoparticles is characterized by eco-friendliness, low cost, ultraviolet-proof, biocompatibility and photocatalysis activity, which could be used to prepare superhydrophobic surface and has potential applications in the field of multifunctional textiles (Yang et al. 2019a, b, c). Yang et al. obtained multifunctional cotton textiles based on PDMS/ZnO composite solution via one-pot dip-coating method (Yang et al. 2019a, b, c). Moreover, some studies reported that ZnO nanoparticle assembled on HNTs could improve photocatalytic activity and absorptivity. Cheng et al. reported an impregnation method to successfully synthesize N-doped ZnO nanoparticle assembled into HNTs, which exhibited remarkable photocatalytic activity compared to pure ZnO nanoparticles (Cheng et al. 2015). So far there is rare report on the facile fabrication of superhydrophobic cotton fabrics with self-cleaning, UV shielding, photocatalysis, and oil/water separation using hierarchical ZnO/HNTs hybrid particles.

In this paper, ZnO/HNTs hybrid particles synthesized via in-situ growth of ZnO on the surface of HNTs were used as the initial building block to prepare robust, superhydrophobic cotton fabrics with self-cleaning, UV shielding, photocatalysis, and oil/water separation. The surface morphologies, chemical composition, wettability, mechanical durability, UV stability, and anti-corrosion, self-cleaning, photocatalysis, and oil/water separation performances of all samples were characterized. These results demonstrated that the obtained multifunctional cotton fabric showed wide application even in harsh environment.

Experimental

Materials

Zinc nitrate ($Zn(NO_3)_2{\cdot}6H_2O$), methylene blue (MB), tetrahydrofuran (THF), ammonium hydroxide ($NH_3.H_2O$,30%) were offered by Sinopharm Chemical Reagent Co. (China). Polydimethylsiloxane (PDMS, Sylgard-184) with the curing agent was purchased from Dow Corning Co. (USA). The halloysite nanotubes (HNTs, purity > 97%) were purchased from Ishu International. Cotton fabrics (plain weave, weight: 163 g/m^2) were purchased from a local clothing factory.

Preparation of ZnO/HNTs nanocomposites

ZnO/HNTs nanocomposites were synthesized via in-situ growth of ZnO on the surface of HNTs by sol–gel method. Firstly, 2 g $Zn(NO_3)_2.6H_2O$ and 0.5 g HNTs

were added into 100 mL of deionized water and were stirred vigorously to form a homogenous solution at room temperature. Then pH of solution was adjusted to 9–10 with $NH_3.H_2O$. The mixed solution was further reacted at 60 °C for 2 h to obtain the ZnO/HNTs sol. After centrifugal washing and drying, a white powder was obtained. Finally, it was calcined in a muffle furnace at 450 °C for 2 h to obtain ZnO/HNTs hybrid particles.

Fabrication of ZnO/HNTs/PDMS@Cotton and PDMS@Cotton

Firstly, appropriate ZnO/HNTs hybrid particles were dispersed in water to form homogeneous solution A. Besides, a certain amount of PDMS and curing agent (The mass ratio of PDMS to curing agent was 10:1) were added to tetrahydrofuran to form solution B. The clean cotton fabric samples were immersed in the solution A and then dried at 80 °C. The obtained cotton fabrics were called as ZnO/HNTs@Cotton. Then the as-prepared ZnO/HNTs@Cotton was dipped in the solution B and then cured at 130 °C for 0.5 h in an oven. The resultant cotton fabrics were named as ZnO/HNTs/PDMS@Cotton. The cotton fabric samples PDMS@Cotton coated by only PDMS was also prepared by the same method.

Sample characterization

The surface morphologies of samples were observed by using scanning electron microscope (SEM, Hitachi S-4800). The element distribution of cotton surface was examined by an energy dispersive spectrometer (EDS, EscaLab Xi+). Chemical groups of samples were identified by Fourier transformer infrared spectrometer (FTIR, Nicolet IS 10, Thermo). Thermogravimetric analysis (TGA) was tested using a thermogravimetric analyzer (Q500, TA). The UV-blocking property of the samples was measured by a Labsphere UV-2000 ultraviolet transmittance analyzer.

Wettability test

The static water contact angles (WCA) of cotton fabric were tested by Krüss DSA 30 (Krüss, Germany). The water shedding angle (WSA) was tested according to reported literature (Wu et al. 2013; Zhang et al. 2013). The average of five values from a same sample which was defined as the final WCA and WSA of the cotton fabric surface.

Durability test

The abrasion resistance of superhydrophobic cotton fabrics was measured by a fabric abrasion tester according to previous literature (Xu et al. 2020). The superhydrophobic cotton fabrics were illuminated under an ultraviolet (UV) lamp of 150 W for 90 h continuously. The contact angles of the ZnO/HNTs/PDMS@Cotton after UV illumination were recorded to evaluate the UV resistance. The chemical stability of coated cotton fabrics was investigated by testing contact angles of coated cotton fabrics after immersing into corrosive liquids with different pH ranging from 1 to 14 for 1 h.

Oil/water separation test and oil absorption test

The oil/water separation experiment of coated cotton fabrics was carried out by using a simple and facile laboratory-made setup. The coated cotton fabric was placed between cylindrical filter funnel and conical flask as filter membrane, and the 100 mL yellow oil and 100 mL blue water mixed solution were poured into the funnel. The separation efficiency (η) was calculated according to $\eta = \frac{M_{After}}{M_{Before}} \times 100\%$, where M_{After} and M_{Before} is the quality of the oil/water mixed solution before and after separation process.

The flux was obtained according to $F = V/St$, where V is the volume of oil permeated coated fabric, S is valid area of the film, and t is the time for collect of V ml of oil.

Photocatalytic activity

The photocatalytic activity of superhydrophobic cotton fabrics with the size of 3 cm×5 cm and other samples were investigated by degrading 10 mg/L methylene blue (MB) solution. To avoid adsorption effects, the samples were magnetically stirred thoroughly in the dark environment until reaching the adsorption–desorption equilibrium of MB with photocatalyst before 150 W UV lamp. Every 30 min, 2 mL of the reaction solution was extracted and centrifuged to remove photocatalyst particles. Then the

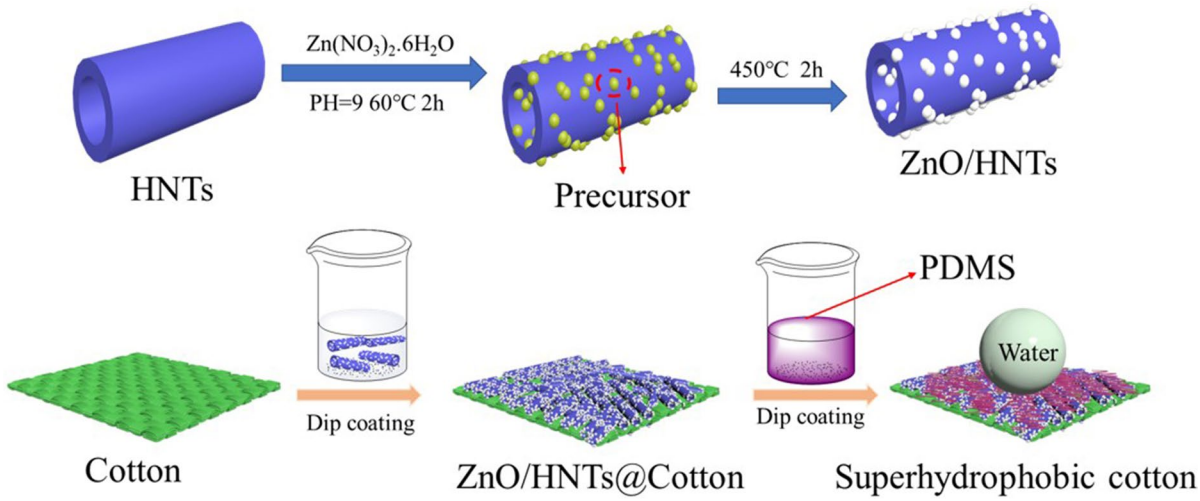

Fig. 1 Schematic diagram of fabrication process of ZnO/HNTs hybrid particles and superhydrophobic fabrics

corresponding absorbance of the characteristic peak at 665 nm was measured by UV–visible absorption spectrum to record the concentration change of MB.

Results and discussion

Preparation of ZnO/HNTs hybrid particles and ZnO/HNTs/PDMS@Cotton

The preparation process of the ZnO/HNTs hybrid particles and ZnO/HNTs/PDMS@Cotton was schematically shown in Fig. 1. First, the Zn^{2+} ionized by $Zn(NO_3)_2.6H_2O$ in the aqueous solution attracted water molecules to form the solvent unit $Zn(H_2O)_2$. The solvent unit released H^+ in an alkaline environment to maintain the coordination number to generate the precursor $Zn(OH)_2$. $Zn(OH)_2$ combined with Al–OH and Si–OH groups on the inner and outer walls of HNTs nanotubes by hydrogen bonding. The active sites on the inner and outer surfaces of the HNTs nanotubes could play a role in dispersing the precursors and prevent the precursors from agglomerating. Subsequently, the precursor-loaded HNTs nanotubes were calcined at a high temperature of 450 °C to obtain ZnO/HNTs nanocomposites. Then, the pristine cotton fabrics were dipped into micro/nano hierarchical ZnO/HNTs hybrid particles dispersion to obtain ZnO/HNTs@Cotton. The ZnO/HNTs hybrid particles dispersion could endow cotton fibers desirable roughness, which could generate micro/nano hierarchical structure combined with the natural morphology of the cellulose fiber. Finally, the ZnO/HNTs@Cotton was modified by PDMS to obtain superhydrophobic cotton fabrics, which could lower the surface tension of ZnO/HNTs@Cotton.

Characterization of ZnO/HNTs hybrid particles and superhydrophobic cotton fabrics

The surface morphologies of HNTs, ZnO/HNTs hybrid particles, PDMS@Cotton and ZnO/HNTs/PDMS@Cotton were observed by SEM. As illustrated in Fig. 2A, HNTs showed a homogeneously nanorod-like structure with a length and a diameter range of 0.7–1.5 μm and 30–50 nm, respectively. Compared with nanorod-like structures of the HNTs, the ZnO/HNTs hybrid particles exhibited unique rod-dot micro/nano hierarchical structures when the ZnO nanoparticles were introduced on surfaces of HNTs (Fig. 2 C, D). PDMS@Cotton fabric showed relative smooth surface, but there were still special folds and grooves in the longitudinal direction (Fig. 2 E, F). In contrast, the ZnO/HNTs/PDMS@Cotton became much rougher, with particulate protrusions compacted on the cotton fabric surface (Fig. 2 G). ZnO/HNTs/PDMS@Cotton was quite densely covered with ZnO/HNTs hybrid particles. The micro/nano hierarchical re-entrant structure caused by ZnO/HNTs hybrid

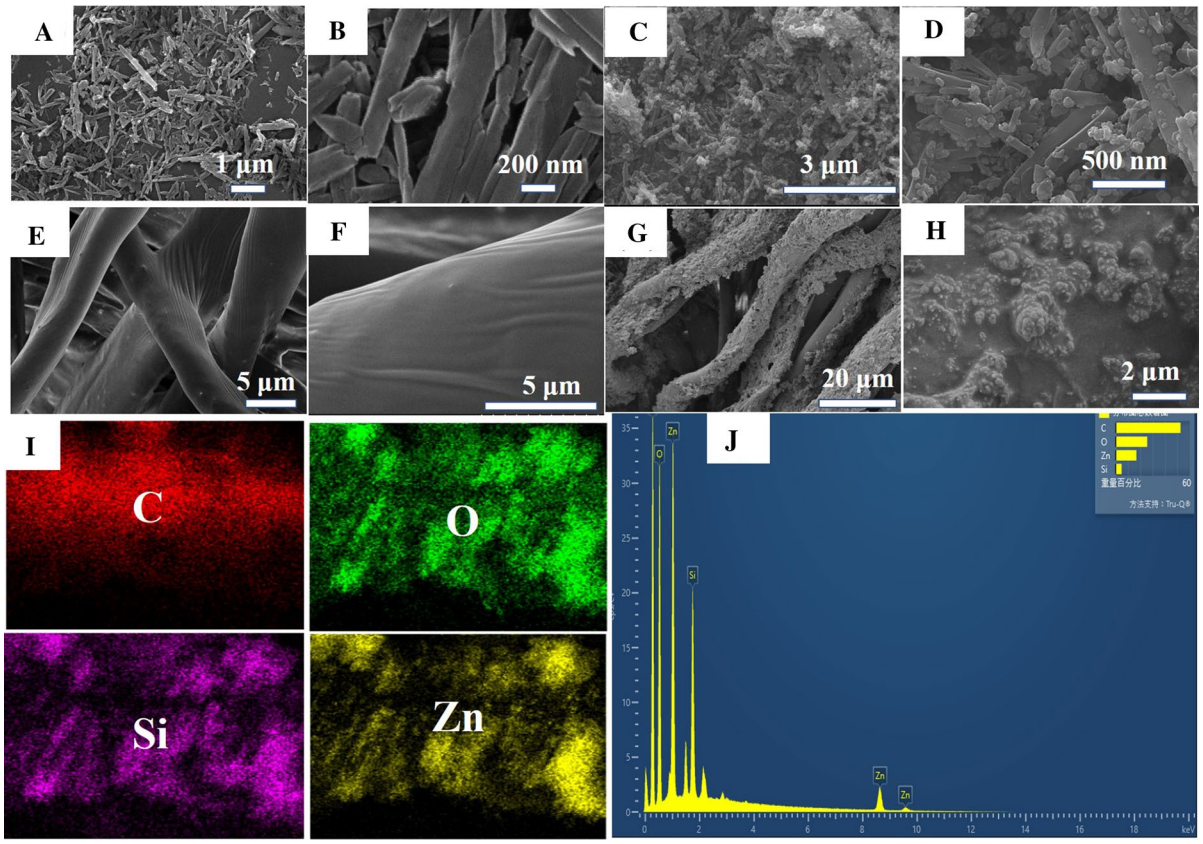

Fig. 2 SEM images: **A, B** HNTs with different magnifications; **C, D** ZnO/HNTs hybrid particles with different magnifications; **E, F** PDMS@Cotton with different magnifications; **G, H** ZnO/HNTs/PDMS@Cotton with different magnifications; EDS **I** Elemental mapping of C, O, Zn and Si for the ZnO/HNTs/PDMS@Cotton; **J** spectrum of the ZnO/HNTs/PDMS@Cotton

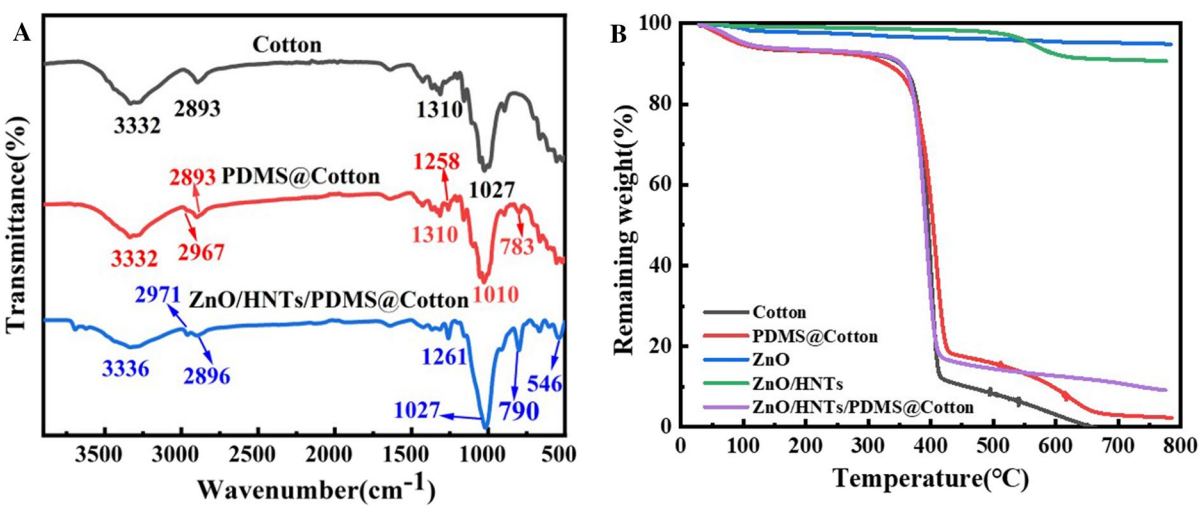

Fig. 3 **A** FTIR spectra of pristine cotton fabrics, PDMS@Cotton and ZnO/HNTs/PDMS@Cotton; **B** TGA curves of ZnO, ZnO/HNTs hybrid particles, pristine cotton fabrics, PDMS@Cotton, and ZnO/HNTs/PDMS@Cotton

particles was constructed on ZnO/HNTs/PDMS@Cotton surface. Moreover, the higher magnification SEM image of ZnO/HNTs/PDMS@Cotton shown in Fig. 2H revealed that ZnO/HNTs coating was covered with a thin layer of PDMS adhesive coating. From Fig. 2G and H, for ZnO/HNTs/PDMS@Cotton, PDMS and ZnO/HNTs hybrid particles were bonded together firmly on cotton fiber surface.

For further investigation of coated cotton fabrics, the chemical components of the pristine cotton fabrics, PDMS@Cotton, and ZnO/HNTs/PDMS@Cotton were characterized by EDS and FTIR. As shown in Fig. 2J, the C, O, Si and Zn elements were distributed on the surface of the coated cotton fabric, suggesting the successful coating of ZnO/HNTs and PDMS on treated cotton fabric surface. ZnO/HNTs/PDMS@Cotton was successfully prepared. In addition, the uniform distribution of C, O, Zn and Si elements indicated that ZnO/HNTs hybrid particles and PDMS were evenly covered on cotton surface (Fig. 2I).

As shown in Fig. 3A, in FTIR spectrum of pristine cotton fabrics, it could be clearly observed from the infrared spectrum that a strong and broad absorption peak appeared at 3332 cm^{-1}, which was the characteristic peak of the stretching vibration of the hydroxyl group in the cellulose macromolecule of the pristine cotton fabrics. Two characteristic absorption peaks could be observed at 2893 cm^{-1} and 1310 cm^{-1}, namely $–CH_3$ stretching vibration and bending vibration absorption. The strongest absorption peak at 1027 cm^{-1} originated from the flexural vibration of the hydroxyl group (–OH) in the cotton cellulose macromolecule and the C–O–C stretching vibration absorption. When the cotton fabrics were coated with PDMS (PDMS@Cotton), new peaks at 2967 cm^{-1}, 1258 cm^{-1}, and 783 cm^{-1} occurred, which were assigned to $–CH_3$ stretching vibration, Si–C bend vibration and Si–O–Si symmetrical stretching vibration, respectively, which were due to a lot of $-CH_3$ groups and Si–O–Si groups of PDMS. The appearance of these characteristic peaks indicated that PDMS had been successfully grafted onto cotton fabrics. Compared with PDMS@Cotton, in FTIR spectra of ZnO/HNTs/PDMS@Cotton additional characteristic peaks appeared at 546 cm^{-1} originating from vibration absorption peak of Al–O–Si, and the Si–O–Si characteristic peak intensity was higher at 790 cm^{-1}, which were ascribed to the appearance of HNTs. The results indicated that the coating composed of ZnO/HNTs hybrid particles and PDMS was successfully incorporated onto cotton fabric.

The thermal stability of the ZnO, ZnO/HNTs hybrid particles, pristine cotton fabric, PDMS@Cotton and ZnO/HNTs/PDMS@Cotton were investigated by thermo gravimetric analysis (TGA). For the TGA curves of ZnO nanoparticles and hierarchical ZnO/HNTs hybrid particles, a very small weight loss occurred from room temperature to 700 °C. The final residual weight percentage of ZnO/HNTs hybrid particles was about 90.637% with heating temperature of 700 °C, indicating that ZnO/HNTs hybrid particles had excellent thermal stability. As shown in Fig. 3B, under the temperature of 350 °C, 11% weight loss of the pristine cotton fabrics was observed, and the weight loss of PDMS@Cotton and ZnO/HNTs/PDMS@Cotton were 13% and 10%, respectively. The weight loss of pristine cotton fabrics, PDMS@Cotton and ZnO/HNTs/PDMS@Cotton from room temperature to 350 °C was small probably caused by moisture evaporation and impurities decomposition absorbed on fabric surface. From 350 °C to 420 °C, the weight loss of pristine cotton fabrics was 78.5% because of the decomposition of cellulose from cotton fabric. Untreated cotton fabric showed residual weight rate of about 0.01% after being heated to 700 °C because of the residual groups (such as $-CH_2-$, etc.) decomposition, indicating that untreated cotton fabric showed almost complete combustion. The remaining weight percentage of PDMS@Cotton after being heated to 700 °C was 2.3%, which was higher than pristine cotton fabric because of the residual groups mainly caused by the incomplete decomposition of PDMS. In contrast, for ZnO/HNTs/PDMS@Cotton after being heated to 700 °C, the residual weight percentage reached to 9.1%, mainly due to the coating composed of ZnO/HNTs and PDMS with excellent thermal stability. TGA of the ZnO, ZnO/HNTs hybrid particles, pristine cotton fabric, PDMS@Cotton and ZnO/HNTs/PDMS@Cotton revealed the successful incorporation of ZnO/HNTs hybrid particles and PDMS on the cotton fabric surface.

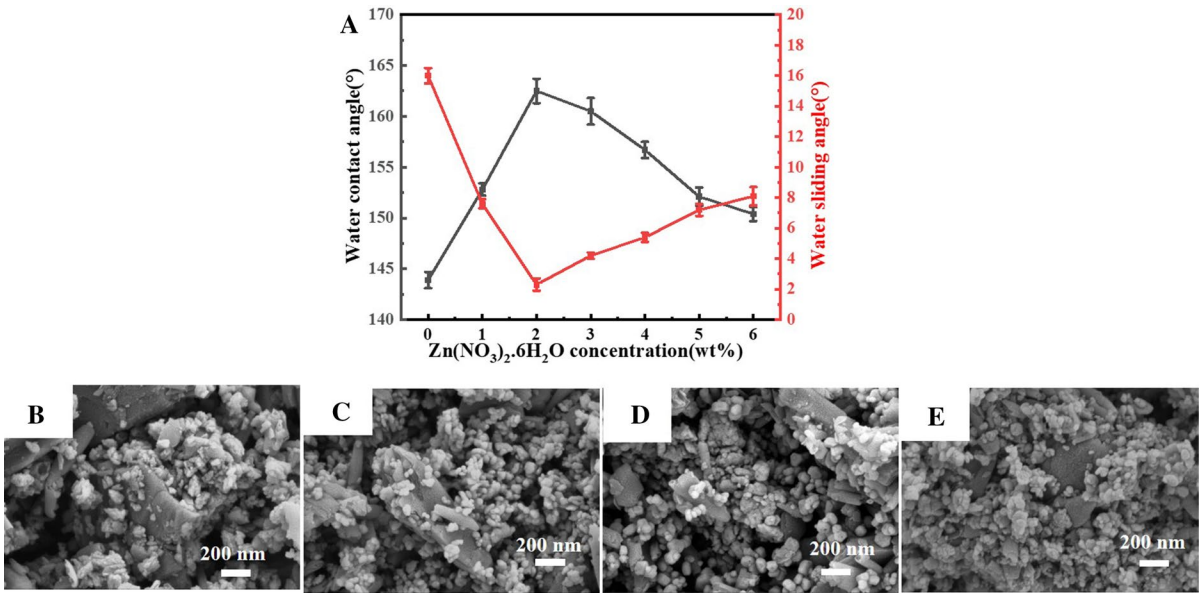

Fig. 4 **A** The effect of $Zn(NO_3)_2.6H_2O$ concentration on the hydrophobicity of ZnO/HNTs/PDMS@Cotton; SEM images of the ZnO/HNTs hybrid particles prepared with $Zn(NO_3)_2.6H_2O$ concentration of **B** 1 wt%; **C** 2 wt%; **D** 3 wt%; **E** 4 wt%

Wettability of superhydrophobic cotton fabrics

Surface roughness and chemical composition are two key factors for preparation of superhydrophobic surface. The superhydrophobicity of the ZnO/HNTs/PDMS@Cotton was affected by microstructures of ZnO/HNTs hybrid particles. For ZnO/HNTs hybrid particles, the used $Zn(NO_3)_2.6H_2O$ concentration showed an impact on microstructure of ZnO/HNTs hybrid particles. The effect of $Zn(NO_3)_2.6H_2O$ concentration on the hydrophobicity of ZnO/HNTs/PDMS@Cotton was shown in Fig. 4A. As displayed in Fig. 4A, the HNTs/PDMS@Cotton exhibited hydrophobicity with WCA of $143.9 \pm 1.2°$. The results indicated that the coating composed of HNTs and PDMS were unable to endow pristine cotton fabric superhydrophobicity. The microstructures of ZnO/HNTs hybrid particles prepared with different $Zn(NO_3)_2.6H_2O$ concentrations were characterized by SEM. When 1 wt% $Zn(NO_3)_2.6H_2O$ was used to prepare ZnO/HNTs hybrid particles, the distribution of ZnO nanoparticles grown on the surface of HNTs was uneven and sparse (Fig. 4B). The surface micro/nano structures of the ZnO/HNTs/PDMS@Cotton with a WCA of $154.7 \pm 1.4°$ obtained based on ZnO/HNTs prepared with $Zn(NO_3)_2.6H_2O$ concentration of 1 wt% was sufficient to support the water droplets in the Cassie-Baxter state. In contrast, When the concentration of $Zn(NO_3)_2{\cdot}6H_2O$ was increased to 2 wt%, the ZnO nanoparticles grown on the surface of HNTs were uniformly distributed, and the average diameter of ZnO nanoparticles was about 15–20 nm (Fig. 4C). The coated cotton fabrics based on ZnO/HNTs hybrid particles prepared with $Zn(NO_3)_2.6H_2O$ concentration of 2 wt% displayed excellent superhydrophobicity with a water contact angle of $162.5 \pm 1.0°$ due to the further enhanced surface roughness. The superhydrophobicity of ZnO/HNTs/PDMS@Cotton obtained based on ZnO/HNTs hybrid particles prepared with further increased $Zn(NO_3)_2.6H_2O$ concentration of 6 wt% was negatively affected, showing water contact angle (WCA) of $150.2 \pm 0.7°$. This was mainly due to the excessive growth of ZnO nanoparticles on the surface of HNTs when concentration of $Zn(NO_3)_2{\cdot}6H_2O$ was higher than 2 wt%. ZnO nanoparticles with high surface energy were easy to agglomerate, leading to the ZnO nanoparticles with larger size densely distributed on HNTs surface (Fig. 4D and E). As a result, the ZnO/HNTs/PDMS@Cotton obtained based on ZnO/HNTs hybrid particles prepared with higher $Zn(NO_3)_2.6H_2O$ concentration showed the decreased surface roughness and lower hydrophobicity. Therefore, $Zn(NO_3)_2.6H_2O$ with mass fraction of 2 wt.% was the optimal choice for subsequent experiments.

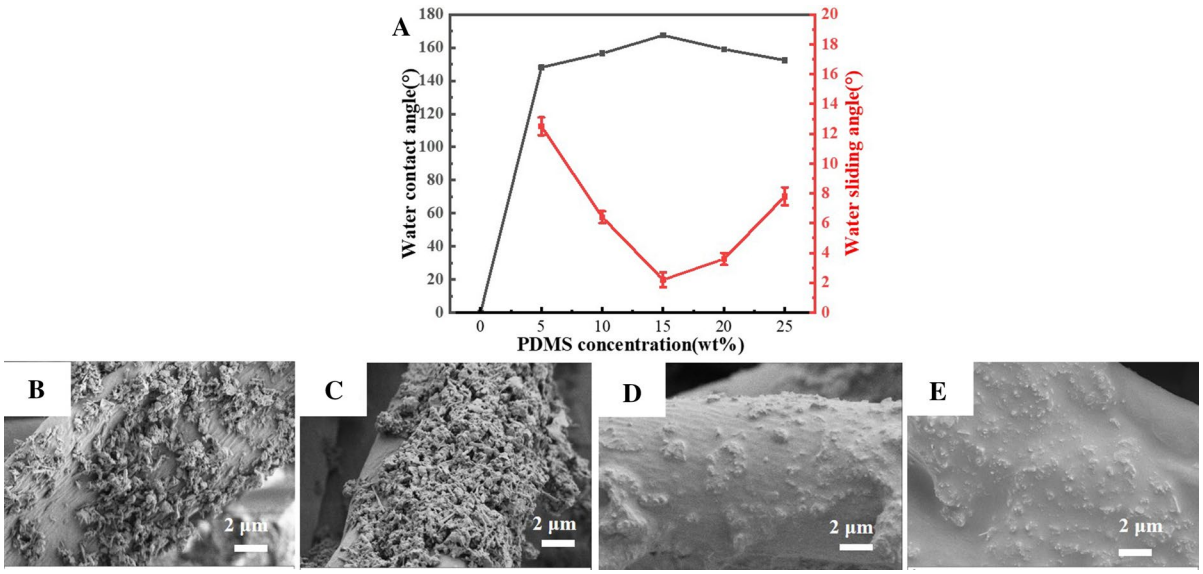

Fig. 5 **A** The effect of PDMS concentration on the hydrophobicity of ZnO/HNTs/PDMS@Cotton; SEM images of the ZnO/HNTs/PDMS@Cotton with PDMS concentration of **B** 5 wt%; **C** 10 wt%; **D** 15 wt%; **E** 20 wt%

The superhydrophobicity of the ZnO/HNTs/PDMS@Cotton was also strongly dependent on the concentration of PDMS. The effect of PDMS concentration on the hydrophobicity of ZnO/HNTs/PDMS@Cotton was shown in Fig. 5A. The microstructures of ZnO/HNTs/PDMS@Cotton prepared with different PDMS concentrations were characterized by SEM (Fig. 5). As shown in Fig. 5A, in the absence of PDMS, the ZnO/HNTs@Cotton was easily wetted due to the inherent hydrophilic properties of the ZnO/HNTs hybrid particles and cellulose. Once 5 wt% of PDMS concentration was introduced, the WCA of ZnO/HNTs/PDMS@Cotton increased dramatically from 0° to 148.1 ± 1.2°. With increasing the concentration of PDMS from 5 wt% to 15 wt%, the WCA increased observably from 148.1 ± 1.2° to 162.5 ± 1.0°. The introduction of proper PDMS concentration reduced the surface tension of ZnO/HNTs/PDMS@Cotton, and didn't significantly affect the micro/nano structure of the coated cotton fabric surface (Fig. 5B–D). The WCA of ZnO/HNTs/PDMS@Cotton slightly decreased with too high concentration of PDMS. The excess PDMS completely covered ZnO/HNTs hybrid particles with hierarchical micro/nano structure when the concentration of PDMS was too high (20 wt%). Consequently, a surface with lower roughness was formed (Fig. 5E), which was consistent with the changes in the WCA of ZnO/HNTs/PDMS@Cotton.

To further evaluate superhydrophobic property of the coated cotton fabric, the Cassie-Baxter model was used to explain the influence of hierarchical rough surface on wettability. According to Cassie-Baxter's equation, the apparent contact angle on the surface(θ^*) is calculated as

$$\cos\theta^* = rf\cos\theta + f - 1 \quad (1)$$

where θ presents the Young's contact angle that is obtained on the slippy surface with the same composition, r is the actual wetted area divided by the projected wetted area of the surface, f is the fraction of the projected area of the solid surface contacting the liquid.

In Eq. (1), r is greater than 1, f is less than 1, and both are positive. The $\theta < 90°$ is due to the natural hydrophilic properties of cotton fabric. Therefore, if f is small enough, θ^* can be greater than 150° according to Eq. (1). One strategy to minimize the f value is to increase the surface roughness of the material, such as flower-like structure, and micro/nano re-entrant structure. As shown in Fig. 6A, after HNTs and PDMS coating, HNTs/PDMS@

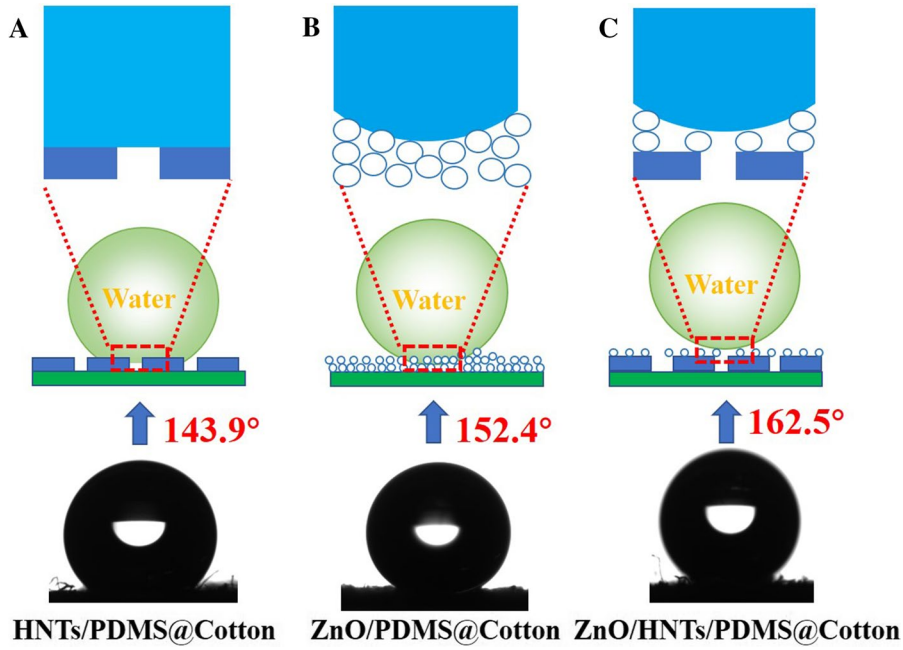

Fig. 6 Different structure wetting states **A** Micro HNTs wetting state; **B** Nano ZnO wetting state; **C** Micro/nano ZnO/HNTs wetting state

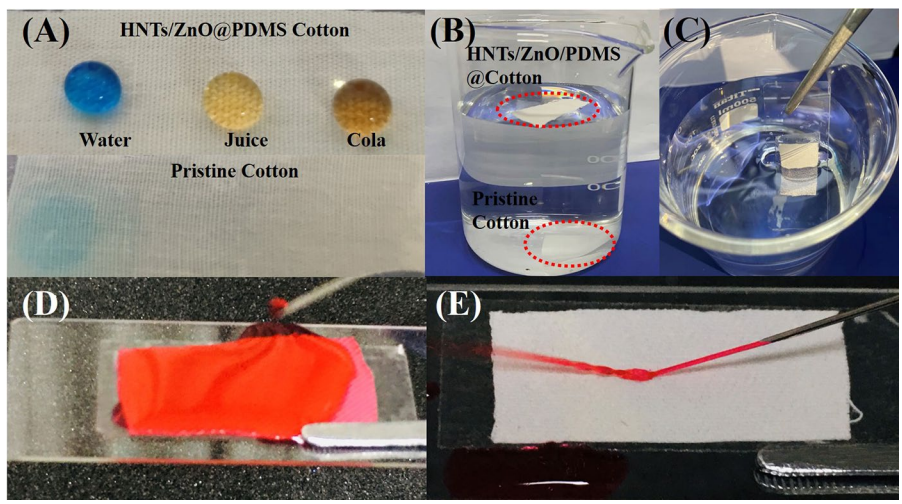

Fig. 7 **A** Different liquid droplets on the surface of the pristine cotton fabric and ZnO/HNTs/PDMS@Cotton; **B** ZnO/HNTs/PDMS@Cotton and pristine cotton fabric in water; **C** immersion of ZnO/HNTs/PDMS@Cotton stuck on glass into water; **D** a jet of colored water spread on the pristine cotton fabric; **E** a jet of colored water was bouncing off from ZnO/HNTs/PDMS@Cotton

Cotton showed hydrophobicity with a WCA of 143.9°. Compared with the microrod-like HNTs stacked coating, the roughness factor of ZnO nanoparticles was increased, showing a certain degree of superhydrophobicity with a WCA of 152.4° (Fig. 6B). In this paper, a micro/nano hierarchical re-entrant structure was constructed by depositing ZnO nanoparticles onto the rod-like HNTs surfaces. As displayed in Fig. 6C, the deposition of ZnO nanoparticles further increased the surface roughness of ZnO/HNTs hybrid particles, resulting in a significant reduction in the liquid/solid contact area. The coated cotton fabrics displayed excellent superhydrophobicity with a water contact angle of 162.5° due to the more trapped air layer.

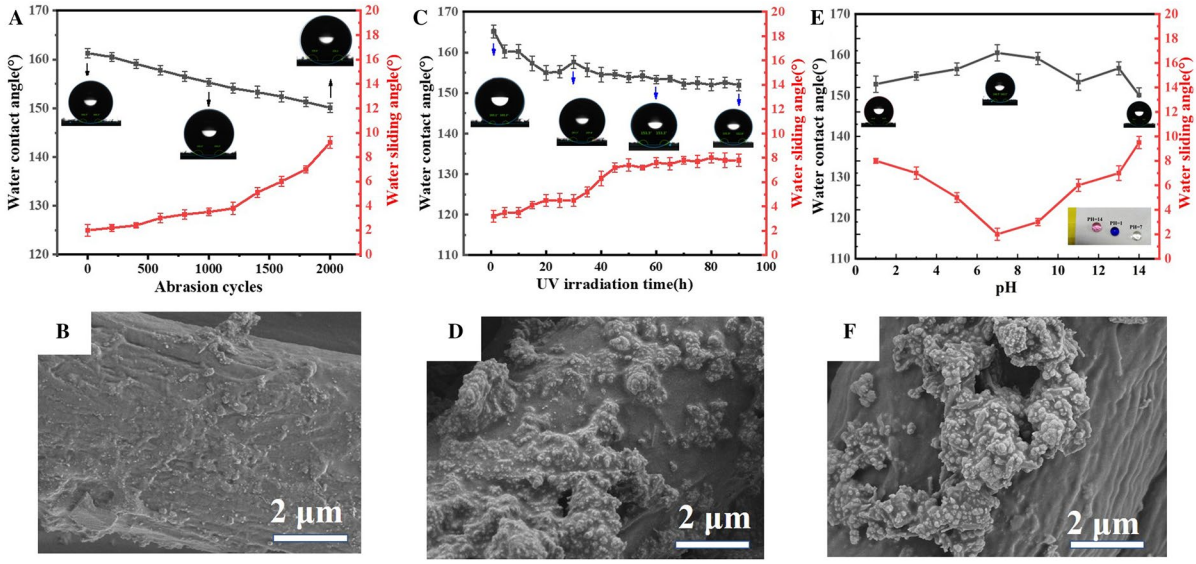

Fig. 8 **A** WCA of ZnO/HNTs/PDMS@Cotton after different abrasion cycles test; **B** SEM image of ZnO/HNTs/PDMS@Cotton after abrasion for 2000 cycles; C WCA of ZnO/HNTs/PDMS@Cotton after different UV irradiation time; **D** SEM image of ZnO/HNTs/PDMS@Cotton after UV irradiation for 90 h; **E** WCA of ZnO/HNTs/PDMS@Cotton after immersion in solution with different pH values; F SEM image of ZnO/HNTs/PDMS@Cotton after immersion in solution with pH value of 14

The surface wettability of superhydrophobic cotton fabrics were analyzed by evaluating their static/dynamic wettability performances. As shown in Fig. 7A, different liquid droplets including blue colored water, juice, and cola were dropped on pristine cotton fabric and ZnO/HNTs/PDMS@Cotton. These aqueous droplets collapsed on the untreated cotton fabric due to its hydrophilic nature. In contrast, the ZnO/HNTs/PDMS@Cotton could hold on all liquid droplets in a spherical shape without any penetration. When the pristine cotton fabric and ZnO/HNTs/PDMS@Cotton were immersed in water, photographs of cotton fabrics were shown in Fig. 7B. The pristine cotton fabrics promptly sank to the bottom of water. However, ZnO/HNTs/PDMS@Cotton could float on water without any wetting. As illustrated in Fig. 7C, when the fixed ZnO/HNTs/PDMS@Cotton was immersed in water, a sliver mirror surface was observed due to the existence of an air cushion surrounded by the coating. Additionally, a jet of red water could easily bounce off from the coated cotton fabric surface without leaving a trace (Fig. 7E). In contrast, a jet of red colored water easily wet on pristine cotton fabrics (Fig. 7D).

Durability evaluation of the superhydrophobic cotton fabrics

In practical applications, most of superhydrophobic coatings easily lose their superhydrophobicity under harsh conditions, such as mechanical abrasion and UV irradiation. As illustrated in Fig. 8A, after 2000 abrasion cycles, the WCA of ZnO/HNTs/PDMS@Cotton showed only slight change, still higher than 150°. The results indicated that the composite coating composed of the silicone elastomer PDMS and ZnO/HNTs hybrid particles on the surface of the cotton fabrics still maintained excellent superhydrophobicity after mechanical abrasion although ZnO/HNTs hybrid particles of the fiber surface was partially destroyed (Fig. 8B). This was attributed to PDMS, which not only lowered the surface energy of the coating, but also formed a dense film on the surface of the cotton fabrics and bonded the ZnO/HNTs hybrid particles tightly on the surface of the cotton fiber to enhance the mechanical durability of superhydrophobic cotton fabric (Guo et al. 2019; Li et al. 2016; Ge et al. 2020). In our study, for ZnO/HNTs/PDMS@Cotton prepared with ZnO/HNTs hybrid particles and PDMS, PDMS played an important role in protecting the coated

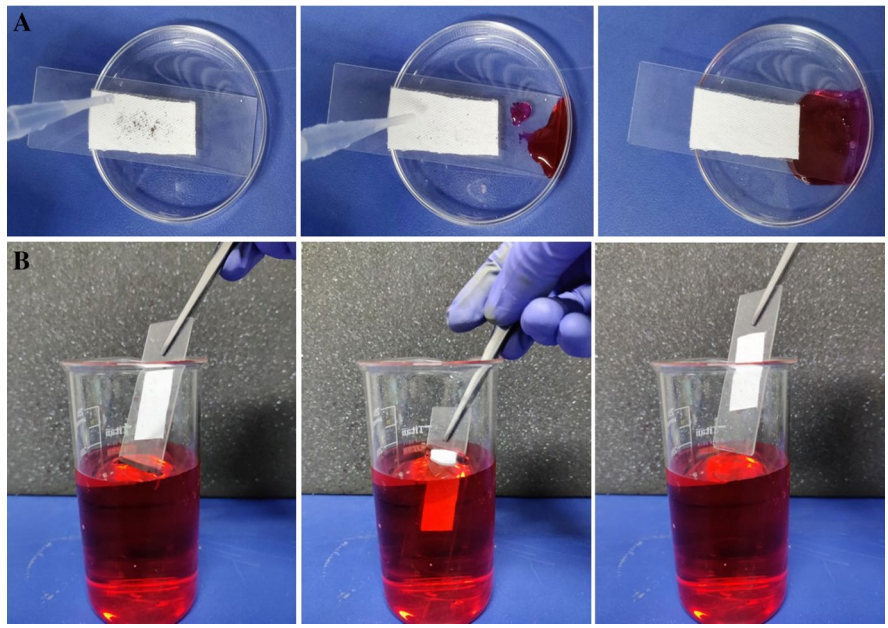

Fig. 9 **A** Self-cleaning property test of ZnO/HNTs/PDMS@Cotton and **B** antifouling property test of ZnO/HNTs/PDMS@Cotton

cotton fabric surface and improving the mechanical properties of the coated fabrics. PDMS as adhesive protective layer firmly adhered to the surface of the coated cotton fabric and ZnO/HNTs hybrid particles, making cotton fibers and ZnO/HNTs hybrid particles tightly bound to each other.

In addition, as presented in Fig. 8C, the WCAs of superhydrophobic cotton fabrics remained around 150° after UV irradiation for 90 h, showing good UV-durability. From Fig. 8D, typical micro/nano hierarchical structure was retained on the microscale fiber surface of ZnO/HNTs/PDMS@Cotton after UV irradiation for 90 h. This was mainly due to the anti-ultraviolet properties of ZnO/HNTs hybrid particles and the strong bond energy of the –Si–O–Si– bond contained in the PDMS layer, which made PDMS resistant to UV decomposition. Moreover, the chemical stability of the coated cotton fabrics was also evaluated. The influence of acid and alkali on the wettability of the superhydrophobic cotton fabrics was tested by immersing in different pH value solutions ranging from 1 to 14 for 1 h. As displayed in Fig. 8E, the WCA of ZnO/HNTs/PDMS@Cotton after dipping in solution with pH value varying from 1 to14 still kept higher than 151°. As shown in Fig. 8F, there were still hierarchical rough morphology on cotton fiber surface of ZnO/HNTs/PDMS@Cotton. The results indicated that the prepared cotton fabrics showed great potential in arousing consumer interest and large-scale industrial applications.

Self-cleaning antifouling performance

Self-cleaning behavior refers to the phenomenon that various contaminants on solid surfaces can be eliminated under natural circumstance. In this study, in order to investigate self-cleaning of the coated cotton fabrics, a layer of methyl red powder was used as contaminant. When a continuous process of water droplets was dropped onto ZnO/HNTs/PDMS@Cotton surface, they quickly rolled off and picked up the dissolved methyl red powder without adhering to it (Fig. 9A). Consequently, the excellent self-cleaning ability of the ZnO/HNTs/PDMS@Cotton was confirmed.

Moreover, in order to demonstrate the excellent antifouling ability of the superhydrophobic cotton fabrics, liquid pollutants experiments were carried out. As presented in Fig. 9B, the ZnO/HNTs/PDMS@Cotton was immersed in red colored aqueous solutions and then taken out. The superhydrophobic cotton fabrics still maintained dry without any residue due to the presence of a layer of air between the surface and the liquid, which protected the cotton fabrics from wetting (Yang et al.2019a, b, c; Qu et al. 2020;

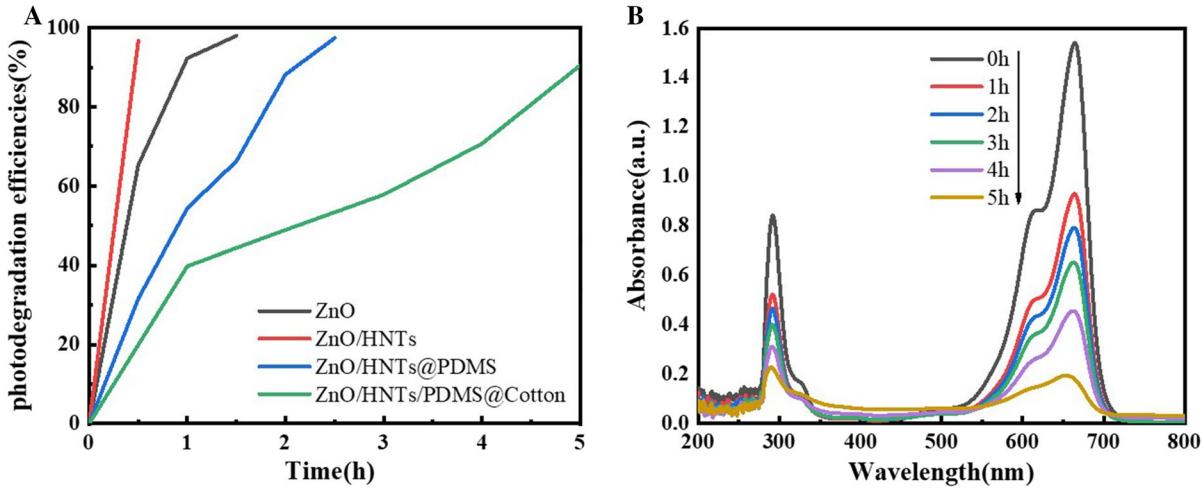

Fig. 10 **A** Photodegradation efficiencies of ZnO/HNTs/PDMS@Cotton and other comparative samples on MB; **B** UV − vis spectra of MB solutions after different irradiation time with the ZnO/HNTs/PDMS@Cotton

Li et al. 2015). Hierarchical rough structures formed by ZnO/HNTs hybrid particles could trap a stable layer of air cushion at the liquid–air-solid interface. The water only could contact the top of the asperities due to the existence of air film, effectively preventing liquid penetration.

Photocatalytic performance

To investigate the photocatalytic degradation of samples, photodegradation experimental toward methyl blue (MB) was carried out. Figure 10A displayed the photodegradation efficiencies of ZnO, ZnO/HNTs hybrid particles, ZnO/HNTs@PDMS, and ZnO/HNTs/PDMS@Cotton toward MB under UV irradiation. Figure 10B gave the UV–vis absorption spectra of MB in ZnO/HNTs/PDMS@Cotton photocatalytic process. As can be seen in Fig. 10A, the ZnO photodegradation efficiencies reached 98% after UV irradiation about 1.5 h. While the absorption bands of MB solution in the presence of the ZnO/HNTs hybrid particles decreased significantly and 96.7% photodegradation efficiencies was obtained after UV irradiation for 0.5 h. The excellent photocatalytic performance of the ZnO/HNTs hybrid particles may be ascribed to the fact that the active sites on the inner and outer surfaces of HNTs hinder the agglomeration of precursors to form smaller-sized ZnO nanoparticles, and HNTs support as adsorbent. Compared with ZnO/HNTs photocatalyst, ZnO/HNTs@PDMS and ZnO/HNTs/PDMS@Cotton needed longer time to achieve the similar photocatalytic efficiencies. Interestingly, ZnO/HNTs@PDMS mostly floated on the surface of methyl blue dilution because of its excellent superhydrophobicity. Undoubtedly, this great superhydrophobicity of ZnO/HNTs@PDMS negatively affected its degradation effect in this experiment. When ZnO/HNTs@PDMS was coated on cotton fabrics, its photocatalytic efficiencies were further reduced. After the ZnO/HNTs/PDMS@Cotton and the MB solution were irradiated by the UV lamp for 5 h, about 90.8% of the MB was degraded. Compared with ZnO/HNTs@PDMS, the contact area between ZnO/HNTs/PDMS@Cotton and methylene blue was further reduced. As can be seen in Fig. 10B, the degradation rate of ZnO/HNTs/PDMS@Cotton to MB gradually decreased with UV irradiation from 0 to 3 h. This could be attributed to the fact that in the range of 0–3 h, as the degradation reaction proceeded, the MB concentration in the system gradually decreased, resulting in the gradual decrease of the contact between ZnO/HNTs/PDMS@Cotton and MB. When the degradation reaction proceeded for 3 h, the degradation rate of ZnO/HNTs/PDMS@Cotton toward MB gradually increased. This could be explained by the fact that as the degradation reaction proceeded, the hydrophobicity of ZnO/HNTs/PDMS@Cotton was getting worse and the contact surface with MB

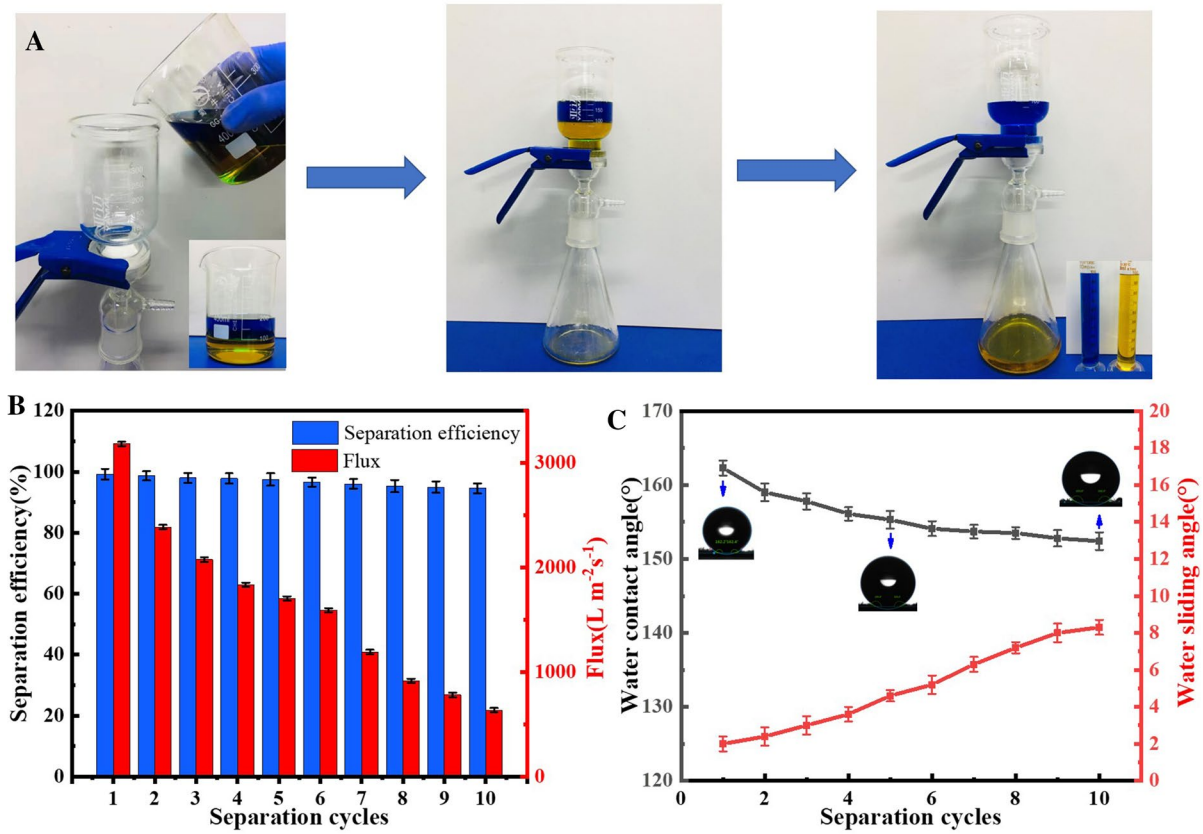

Fig. 11 ZnO/HNTs/PDMS@Cotton: **A** oil/water separation process; **B** separation efficiency and separation flux after different separation cycles; **C** WCA after different separation cycles

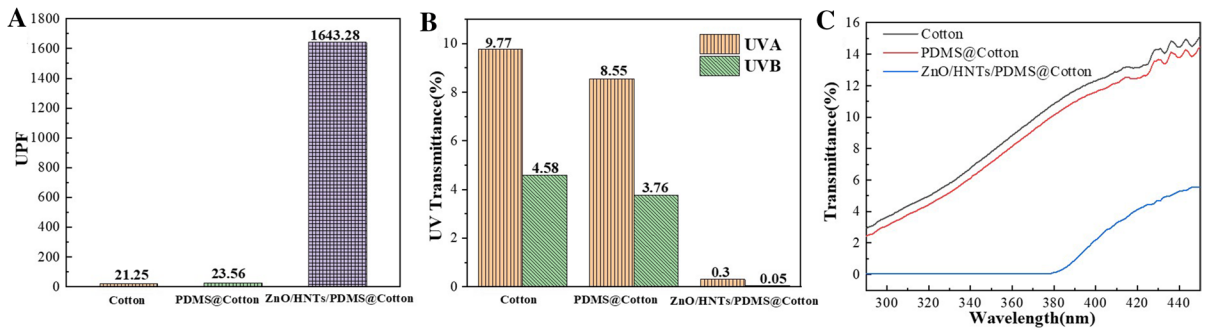

Fig. 12 Pristine cotton fabric, PDMS@Cotton and ZnO/HNTs/PDMS@Cotton: **A** UV transmittance curves, **B** UPF values, and **C** UV transmittance

gradually became larger, and this effect was greater than the reduction of MB concentration in the system on the degradation reaction.

Oil–water separation of the superhydrophobic cotton fabrics

The ZnO/HNTs/PDMS@Cotton possessed both superhydrophobic and superoleophilic characteristics and had a certain application for the separation of oil/water mixtures. Herein, dichloromethane was used to measure the oil/water separation ability of the ZnO/HNTs/PDMS@Cotton. Figure 11A showed the separation processes of dichloromethane by the as-prepared cotton fabric. As expected, while the dichloromethane/water mixture was poured into the filter apparatus, yellow dichloromethane could permeate through the superhydrophobic cotton fabrics filter membrane instantaneously due to gravity, leaving only the water above the filter. After 10 cycles of separation, the superhydrophobic cotton fabrics still exhibited high separation efficiency, and the separation efficiency and flux of dichloromethane/water mixture was up to 94.6% and 636 Lm^{-2} s^{-1}, respectively, indicating excellent recyclability (Fig. 11B). As displayed in Fig. 11C, with the increase of oil/water separation cycles, WCA of ZnO/HNTs/PDMS@Cotton decreased slightly but remained above 150°. These results above mentioned demonstrated that ZnO/HNTs/PDMS@Cotton showed wide application prospects in the field of oil/ water separation.

UV-shielding property of the superhydrophobic cotton fabrics

Figure 12 showed the ultraviolet transmittance spectra and UPF values of pristine cotton fabric, PDMS@Cotton, and ZnO/HNTs/PDMS@Cotton. From Fig. 12, pristine cotton fabrics and PDMS@Cotton displayed similar transmittances curves and didn't show UV shielding performance. In comparison, ZnO/HNTs/PDMS@Cotton exhibited excellent UV shielding effect. UPF value was significantly improved to 1643.28 and UV transmittances of UVA and UVB were only 0.3% and 0.05%, respectively. This result was attributed to strong ultraviolet-absorption, light scattering and frequent light reflection of ZnO nanoparticles in ZnO/HNTs hybrid particles coated on cotton fabrics (Momen et al. 2012).

Conclusion

In summary, hierarchical ZnO/HNTs hybrid particles and PDMS were used to prepare robust, ultraviolet-proof superhydrophobic cotton fabrics with self-cleaning, photocatalysis, and oil/water separation via a facile approach. When the mass fraction of $Zn(NO_3)_2.6H_2O$ and PDMS were 2 wt% and 15 wt%, respectively, the prepared coated cotton fabrics achieved superhydrophobicity with a WCA of $162.5 \pm 1.0°$. Moreover, the superhydrophobic fabrics displayed desirable self-cleaning, antifouling, photocatalysis, and oil/water separating performance. The prepared functional cotton fabrics also demonstrated excellent ultraviolent-proof performance. Importantly, the superhydrophobic cotton fabrics were stable enough to withstand mechanical abrasion test, chemical corrosion, and UV irradiation. This work provided a low cost and environmentally friendly approach for development of multifunctional textiles, which could be employed in self-cleaning, degradation of dye waste and UV shielding fields.

Acknowledgments This work was financially supported by Shanghai Natural Science Foundation (21ZR426200) and National Natural Science Foundation of China (51703123).

Funding This work was financially supported by Shanghai Natural Science Foundation (21ZR426200) and National Natural Science Foundation of China (51703123).

Declarations

Conflict of interest The authors declare that they have no conflict of interest.

References

Banerjee S, Dionysios DD, Pillai SC (2015) Self-cleaning applications of TiO2 by photo-induced hydrophilicity and photocatalysis. Appl Catal B-Environ 176:396–428. https://doi.org/10.1016/j.apcatb.2015.03.058

Cao CY, Ge MZ, Huang JY, Li SH, Deng S, Zhang SN, Chen Z, Zhang KQ, Al-Deyab SS, Lai YK (2016) Robust fluorine-free superhydrophobic PDMS-ormosil@fabrics for highly effective self-cleaning and efficient oil-water

separation. J Mater Chem A 4:12179–12187. https://doi.org/10.1039/c6ta04420d
Cheng ZL, Sun W (2015) Preparation of N-doped ZnO-loaded halloysite nanotubes catalysts with high solar-light photocatalytic activity. Water Sci Technol 72:1817–1823. https://doi.org/10.2166/wst.2015.403
Gang W, Guo ZG, Liu WM (2017) Biomimetic polymeric superhydrophobic surfaces and nanostructures: from fabrication to applications. Nanoscale 9:3338–3366. https://doi.org/10.1039/c7nr00096k
Gao SW, Dong XL, Huang JY, Li SH, Chen Z, Lai YK (2017) Rational construction of highly transparent superhydrophobic coatings based on a non-particle, fluorine-free and water-rich system for versatile oil-water separation. Chem Eng J 333:621–629. https://doi.org/10.1016/j.cej.2017.10.006
Ge MZ, Cao CY, Liang FH, Liu R, Zhang Y, Zhang W, Zhu TX, Yi B, Tang YX, Lai YK (2020) "PDMS-in-water" emulsion enables mechanochemically robust superhydrophobic surfaces with self-healing nature. Nanoscale Horizons 5(1):65–73. https://doi.org/10.1039/C9NH00519F
Guo HS, Yang J, Xu T, Zhao WQ, Zhang JM, Zhu YN, Wen CY, Li QS, Sui JX, Zhang L (2019) A robust cotton textile-based material for high flux oil-water separation. ACS App Mater Inter 11(14):13704–13713. https://doi.org/10.1021/acsami.9b01108
Jiang B, Zhang HJ, Sun YL, Zhang LH, Xu LD, Hao L, Yang HW (2017) Covalent layer-by-layer grafting (LBLG) functionalized superhydrophobic stainless steel mesh for oil/ water separation. Appl Surf Sci 406:150–160. https://doi.org/10.1016/j.apsusc.2017.02.102
Jin M, Feng X, Feng L, Sun T, Zhai J, Li T, Jiang L (2005) Superhydrophobic aligned polystyrene nanotube films with high adhesive force. Adv Mater 17:1977–1981. https://doi.org/10.1002/adma.200401726
Jin GW, Kim JY, Min BG (2018) Superhydrophobic and antibacterial properties of cotton fabrics treated with PVDF and nano-ZnO through phase inversion process. Fiber Polym 19:1835–1842. https://doi.org/10.1007/s12221-018-8313-x
Kim M, Kim K, Lee NY, Shin K, Kim YS (2007) A simple fabrication route to a highly transparent superhydrophobic surface with a poly(dimethylsiloxane) coated flexible mold. Chem Commun 22:2237–2239. https://doi.org/10.1039/b618123f
Kim JH, Mirzaei A, Hyoun W (2018) Novel superamphiphobic surfaces based on micro-nano hierarchical fluorinated Ag/SiO_2 structures. App Surf Sci 445:262–271. https://doi.org/10.1016/j.apsusc.2018.03.148
Li BC, Zhang JP, Gao ZQ, Wei QY (2016) Semitransparent superoleophobic coatings with low sliding angles for hot liquids based on silica nanotubes. J Mater Chem A 4:953–960. https://doi.org/10.1039/C5TA08733C
Li SH, Huang JY, Ge MZ, Cao CY, Deng S, Zhang SN, Chen GQ, Zhang KQ, Al-Deyab SS, Lai YK (2015) Self-cleaning cotton: robust flower-like TiO2@cotton fabrics with special wettability for effective self-cleaning and versatile oil/water separation. Adv Mater Interfaces. https://doi.org/10.1002/admi.201570068
Lin M, Parida K, Cheng X (2017) Flexible superamphiphobic film for water energy harvesting. Adv Mater Technol-Us 2:1600186. https://doi.org/10.1002/admt.201600186
Lin DM, Zeng XR, Li HQ, Lai XJ (2018) Facile fabrication of superhydrophobic and flame-retardant coatings on cotton fabrics via layer-by-layer assembly. Cellulose 25:3135–3149. https://doi.org/10.1007/s10570-018-1748-9
Liu XR, Wang KL, Zhang W, Zhang JP, Li JZ (2019) Robust, self-cleaning, anti-fouling, superamphiphobic soy protein isolate composite films using spray-coating technique with fluorinated HNTs/SiO_2. Compos Part B-Eng 174:107002. https://doi.org/10.1016/j.compositesb.2019.107002
Ma W, Higaki YJ, Takahara A (2017) Superamphiphobic coatings from combination of a biomimetic catechol-bearing fluoropolymer and halloysite nanotubes. Adv Mater Interfaces 4:1700907. https://doi.org/10.1002/admi.201700907
Ma W, Wu H, Higaki YJ, Takahara A (2018) Halloysite nanotubes: green nanomaterial for functional organic-inorganic nanohybrids. Chem Rec 18:986–999. https://doi.org/10.1002/tcr.201700093
Martin JW, Mabury SA, Solomon KR (2003a) Bioconcentration and tissue distribution of perfluorinated acids in rainbow trout (oncorhynchus mykiss). Environ Toxicol Chem 22:196–204. https://doi.org/10.1002/etc.5620220126
Martin JW, Mabury SA, Solomon KR, Muir DCG (2003b) Dietary accumulation of perfluorinated acids in juvenile rainbow trout (Oncorhynchus mykiss). Environ Toxicol Chem 22:189–195. https://doi.org/10.1002/etc.5620220125
Momen G, Farzaneh M (2012) A ZnO-based nanocomposite coating with ultra-water repellent properties. Appl Surf Sci 258:5723–5728. https://doi.org/10.1016/j.apsusc.2012.02.074
Qu MN, Ma XR, Hou LG, Yuan MJ, He J, Xue MH, Liu XG, He JM (2018) Fabrication of durable superamphiphobic materials on various substrates with wear-resistance and self-cleaning performance from kaolin. Appl Surf Sci 456:737–750. https://doi.org/10.1016/j.apsusc.2018.06.194
Qu XF, Cai JB, Tian JH, Luo BH, Liu MX (2020) Superamphiphobic surfaces with self-cleaning and antifouling properties by functionalized chitin nanocrystals. Acs Sustain Chem Eng 8(17):6690–6699. https://doi.org/10.1021/acssuschemeng.0c00340
Rezaei S, Manoucheri I, Moradian R, Pourabbas B (2014) One-step chemical vapor deposition and modification of silica nanoparticles at the lowest possible temperature and superhydrophobic surface fabrication. Chem Eng J 252:11–16. https://doi.org/10.1016/j.cej.2014.04.100
Shishodiaa A, Aroraa HS, Babua A, Mandalb P, Grewala HS (2019) Multidimensional durability of superhydrophobic self-cleaning surface derived from rice-husk ash. Prog Org Coat 136:105221. https://doi.org/10.1016/j.porgcoat.2019.105221
Tu YY, Zou HL, Lin SD, Hu JW (2017) Understanding the mechanism for building woven fabrics with wettability ranging from superhydrophobic to superamphiphobic via an aqueous process. React Funct Polym 119:75–81. https://doi.org/10.1016/j.reactfunctpolym.2017.08.004
Wang WJ, Liu RP, Chi HJ, Zhang T, Xu ZG, Zhao Y (2019) Durable superamphiphobic and photocatalytic fabrics: tackling the loss of super-non-wettability due to surface

organic contamination. ACS Appl Mater Inter 11:35327–35332. https://doi.org/10.1021/acsami.9b12141

Wen BN, Peng S, Yang XJ, Long MY, Deng WS, Chen GY, Chen JQ, Deng WL (2017) A cycle-etching approach toward the fabrication of superamphiphobic stainless steel surfaces with excellent anticorrosion properties. Adv Eng Mater 19:1600879. https://doi.org/10.1002/adem.201600879

Wu L, Zhang JP, Li BC (2013) Mimic nature, beyond nature: facile synthesis of durable superhydrophobic textiles using organosilanes. J Mater Chem B 1:4756–4763. https://doi.org/10.1039/c3tb20934b

Xu LH, Liu YD, Yuan XL, Wan J, Wang LM, Pan H, Shen Y (2020) One-pot preparation of robust, ultraviolet-proof superhydrophobic cotton fabrics for self-cleaning and oil/water separation. Cellulose 27:9005–9026. https://doi.org/10.1007/s10570-020-03369-2

Yang MP, Liu WQ, Jiang C, Liu CH, He S, Xie YK, Wang ZF (2018) Facile preparation of robust superhydrophobic cotton textile for self-cleaning and oil-water separation. Ind Eng Chem Res 58:187–194. https://doi.org/10.1021/acs.iecr.8b04433

Yang MP, Jiang C, Liu WQ, Liang LY, Pi K (2019a) A less harmful system of preparing robust fabrics for integrated self-cleaning, oil-water separation and water purification. Environ Pollut 255:113277. https://doi.org/10.1016/j.envpol.2019.113277

Yang MP, Liu WQ, Jiang C, Xie KY, Shi HY, Zhang FY (2019b) Facile fabrication of robust fluorine-free superhydrophobic cellulosic fabric for self-cleaning, photocatalysis and UV shielding. Cellulose 26:8153–8164. https://doi.org/10.1007/s10570-019-02640-5

Yang MP, Liu WQ, Jiang C, Xie YK, Shi HY, Zhang FY, Wang ZF (2019c) Facile construction of robust superhydrophobic cotton textiles for effective UV protection, self-cleaning and oil-water separation. Colloids Surfaces A 570:172–181. https://doi.org/10.1016/j.colsurfa.2019.03.024

Zhang JP, Li BC, Wu L, Wang AQ (2013) Facile preparation of durable and robust superhydrophobic textiles by dip coating in nanocomposite solution of organosilanes. Chem Commun 49:11509–11511. https://doi.org/10.1039/c3cc43238f

Zhang DQ, Williams BL, Shrestha SB, Nasir Z, Becher EM, Lofink BJ, Santos VH, Patel H, Peng XH, Sun LY (2017a) Flame retardant and hydrophobic coatings on cotton fabrics via sol-gel and self-assembly techniques. J Colloid Interf Sci 505:892–899. https://doi.org/10.1016/j.jcis.2017.06.087

Zhang JP, Gao ZQ, Li LX, Li BC, Sun HX (2017b) Waterborne nonfluorinated superhydrophobic coatings with exceptional mechanical durability based on natural nanorods. Adv Mater Interfaces 4:1700723. https://doi.org/10.1002/admi.201700723

Zhang XT, Liu SQ, Salim A, Seeger S (2019) Hierarchical structured multifunctional self-cleaning material with durable superhydrophobicity and photocatalytic functionalities. Small 15(34):1901822. https://doi.org/10.1002/smll.201901822

Zheng LZ, Su XJ, Lai XJ, Chen WJ, Li HQ, Zeng XR (2019) Conductive superhydrophobic cotton fabrics via layer-by-layer assembly of carbon nanotubes for oil-water separation and human motion detection. Mater Lett 253:230–233. https://doi.org/10.1016/j.matlet.2019.06.078

Zhou QQ, Chen GQ, Xing TL (2018) Facile construction of robust superhydrophobic tea polyphenol/Fe@cotton fabric for self-cleaning and efficient oil–water separation. Cellulose 25:1513–1525. https://doi.org/10.1007/s10570-018-1654-1

Zuo H, Chen L, Kong M, Qiu LP, Wu P, Yang YH, Chen KP (2018) Toxic effects of fluoride on organisms. Life Sci 198:18–24. https://doi.org/10.1016/j.lfs.2018.02.001